Korean J. Chem. Eng., **29**(9), 1266-1271 (2012)
DOI: 10.1007/s11814-011-0303-2

Modeling studies on the effects of the process parameters in forced-flow chemical vapor infiltration reactor for the preparation of C/C composites

Dong Geun Hwang and Gui Yung Chung†

Department of Chemical Engineering, Hongik University, 72-1, Sangsu-dong, Mapo-gu, Seoul 121-791, Korea
(*Received 30 August 2011 • accepted 31 December 2011*)

Abstract−The mathematical modeling for the preparation of C/C composites from propane by F-CVI (Forced-flow chemical vapor infiltration) was studied. Experimental data were fitted with the modeling calculations and an adjusted reaction rate constant was obtained. Effects of many operation parameters such as temperature, the inlet concentration of propane, flow rate, and the initial porosity were observed. The decrease of the deposition rate due to the decrease of porosity and the depletion of propane in the middle of the preform was compensated with the increase of the lateral surface area of fibers. It was confirmed that a slow reaction rate with a low temperature and a low concentration is necessary for a uniform infiltration. As the gas flow rate and the initial porosity increase, the amount of deposition increases.

Key words: C/C Composites, CVI, Propane, Numerical Modeling, Process Parameter

INTRODUCTION

Ceramics have many good properties such as hardness, wear resistance, and non-corrosiveness. Ceramic composites can be produced with these good properties of each component. Chemical vapor infiltration (CVI) is one of many methods for preparing ceramic composites. In CVI, the precursor gas diffuses into a porous perform, reacts at pore walls, and deposits matrix materials [1,2]. It can produce large pieces of composites with complex shapes at the same time.

In case the carbon matrix is filled in a carbon preform, it is called a carbon/carbon composite. Types of preform can be chopped fibers, long cylindrical fibers, and layers of woven fabrics. Modeling of fiber-reinforced ceramic composites by CVI has been studied by many researchers [3-6]. Chung et al. [7-10] studied the mathematical modeling of manufacturing ceramic composites reinforced with multilayer woven fabrics. The numerical simulations were used to optimize parameters of the F-CVI process [11,12]. The detailed kinetic modeling of gas phase reactions [13] and a heterogeneous kinetic modeling of surface reactions in CVI of pyrocarbon by propane pyrolysis [14] were studied. Langhoff et al. modeled CVI of pyrolytic carbon as moving boundary problem [15], and Ibrahim et al. obtained a transient solution of CVI/deposition in a reactor [16].

The objective of this work was the modeling the preparation of woven fiber reinforced C/C composites by F-CVI of carbon from propane. Effects of several parameters of infiltration reaction could be predicted by mathematical modeling. Time changes of pore size, porosity, and amount of deposition were calculated. Times of plugging pore entrances were also estimated.

MODEL DEVELOPMENT

The cylindrical preform is composed of woven fibers. Fibers are assumed nonporous. It is also assumed that pores distributed evenly in the whole preform as shown in Fig. 1 on condition that the total porosity is same as that of a preform used in the experiment.

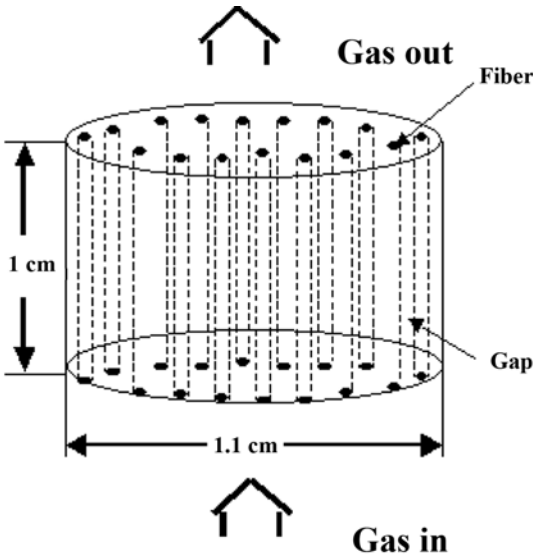

Fig. 1. Schematic diagram of the preform.

Reactant gas, i.e., propane, flows from one side of the preform to another by forced convection in an isothermal reactor. For the gas concentration distribution, a pseudo-steady state was assumed. It is supposed that the carbon deposition reaction is a first-order reaction of propane by which 1 mole propane produces 3 mole carbon and 4 mole H_2 [17].

$$C_3H_8 \rightarrow 3C+4H_2 \quad (1)$$

There is a z-directional convection in the pores among fibers. Following the reaction equation, the mole balance of each component was made.

†To whom correspondence should be addressed.
E-mail: gychung@hongik.ac.kr

$$\frac{1}{A}\frac{\partial QC_A}{\partial Z} - 2\upsilon_A \pi W k_s r_f C_A = 0 \quad (2)$$

b.c. at z=0, $C_A = C_{Ao}$

Here, the first item is the convection flow and the second item is the deposition on the lateral surfaces of fibers in the preform. The deposition rate constant reported by Vaidyaraman [18] was used. They reported 23.6 kcal/mol of activation energy, which is smaller than those in the reference, 48-60 kcal/mol [19].

$$\ln(k_s) = 2.2 - \frac{23,610}{RT} \quad (3)$$

An adjusting value was obtained in the process of fitting calculation results with the experimental data. k_s was multiplied by this value for the model calculations. The momentum balance equation for the packed column was used. The equation for the changes of fiber radius due to deposition is as follows:

$$\frac{\partial r_{fz}}{\partial t} = \frac{qM_m}{\rho_m} k_s C_{Az} \quad (4)$$

i.e., At t=0, $r_f = r_{fo}$

Equations for the amount of deposition per unit cross-sectional area of the preform and porosity are as follows:

$$D_z = \pi \sum_{z=0}^{L} (r_{fz}^2 - r_{fo}^2) \Delta z W \rho_m \quad (5)$$

$$\varepsilon_z = 1 - \pi r_{fz}^2 W \quad (6)$$

The above equations were changed into a dimensionless form with dimensionless parameters, such as $\sigma(=r_f/r_{fo})$ and $\xi(=z/L)$, and solved in a finite difference method. Porosity, the mole fraction of propane, fiber radius, and the amount of infiltration were calculated. After pore entrances were plugged, i.e., the radii of fibers at pore entrances become r_p, the deposition on the outside surface area of the preform was calculated.

RESULTS AND DISCUSSION

Mathematical modeling was carried out with the parameter values listed in Table 1 and the reaction rate constant (k_s) in Eq. (3). Dimensions of the preform were taken from a sample used in the experiment done in our laboratory. Changes of the concentration of propane, porosity, and the amount of deposition were estimated with the mathematical modeling.

1. Data Fitting of the Amount of Deposition

Time changes of the amount of deposition at different inlet percentages of propane are in Fig. 2. Symbols are experimental data and curves are model calculation results. The model calculation results have inflection points when pore entrances are plugged. There is no deposition on the lateral surfaces of cylindrical fibers after the inflection points, and the deposition occurs only on the outside of the preform. The area of the outside surface area of the preform is very small compared with the lateral surface area of cylindrical fibers. So the slopes become small after the inflection points.

Table 1. Characteristics of the preform used in the modeling

Dimensions	1 cm×1 cm×1 cm (L=1 cm, D=1.11 cm)
Porosity	0.617
Average mass	0.48 g
Fiber radius (r_o)	3.5 μm
Fiber radius at the plugging time (r_p)	5.4 μm
Number of fibers per unit cross-sectional area (W)	995,206 cm^{-2}

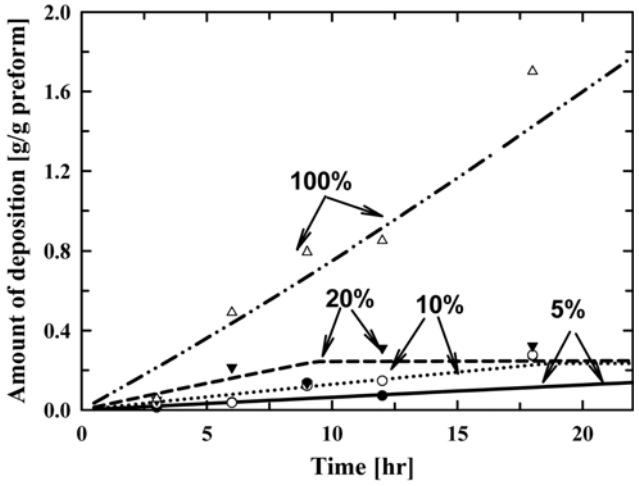

Fig. 2. Comparisons of the modeling calculations with the experimental data of the amount of deposition per unit mass of the preform at different inlet percentages of propane. Modeling calculations were made with $2k_s$ for 100% and $30k_s$ for 5, 10, and 20% propane.

Modeling calculations were fitted to the experimental data with an adjusting parameter. The obtained adjusting parameters were 2 for 100%, 30 for 5, 10, and 20% of the inlet propane. This means that more deposition appears than predicted with the k_s value reported by Vaidyaraman [18]. The possible reason of this is that there might remain open pore entrances in the real preform after the time of plugging pore entrances. An adjusting parameter of 10 was used for the following model calculations.

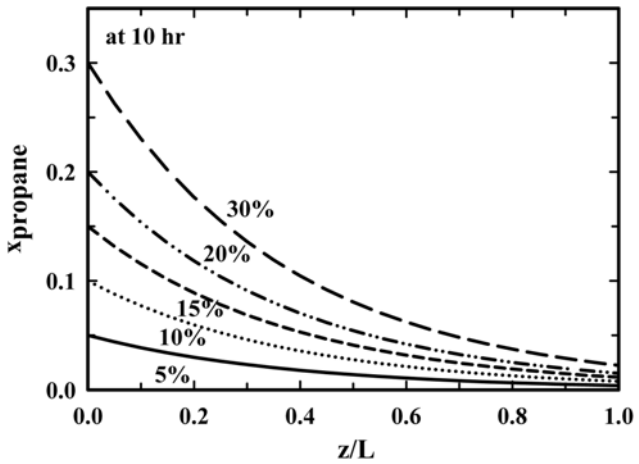

Fig. 3. Changes of the amount of deposition per unit mass of the preform with time at different inlet concentrations of propane.

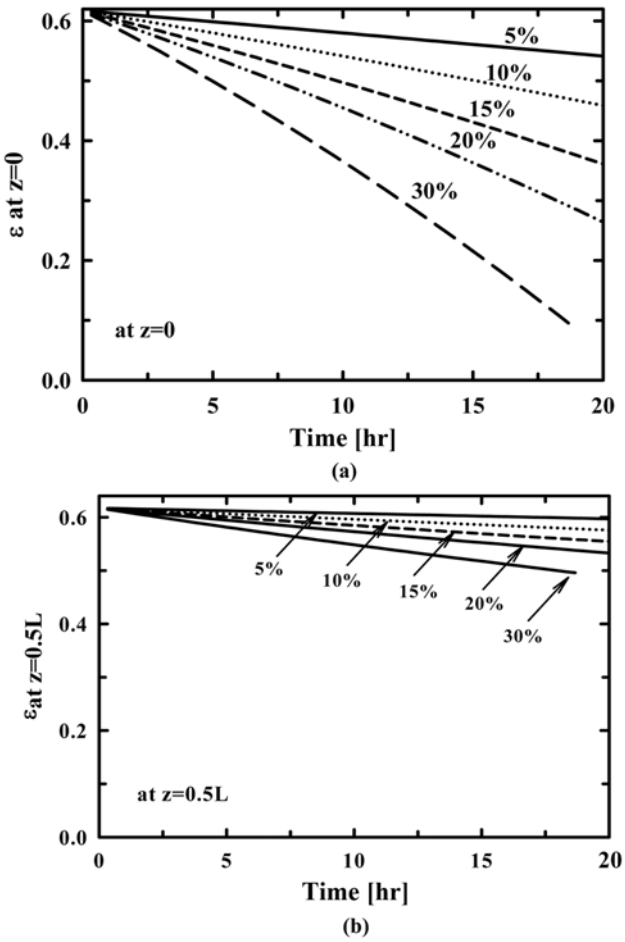

Fig. 4. Time changes of porosity (a) at z=0 and (b) at z=0.5 L in the preform at different inlet concentrations of propane.

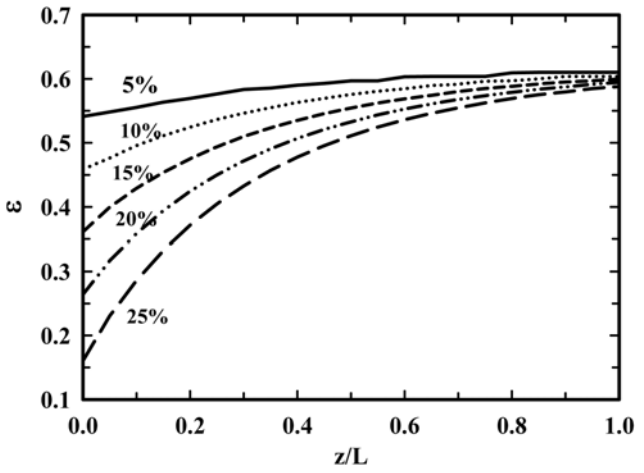

Fig. 5. Porosity distributions in the preform at different inlet propane concentrations at 20 hr and 900 °C.

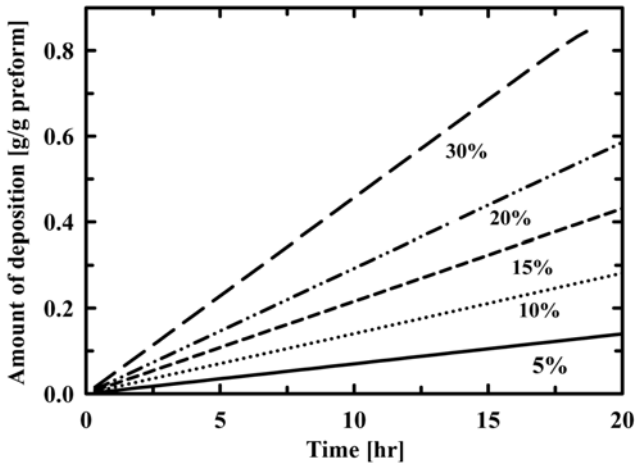

Fig. 6. Time changes of the amount of deposition per unit mass of the preform at different concentrations of propane.

2. Effects of the Concentration of Propane

The concentration of propane decreases along the direction of gas flow because of the depletion of propane due to a deposition reaction. The distributions of the concentration of propane along the direction of gas flow, i.e., z-direction in the preform, at different inlet propane concentrations, are in Fig. 3. The decreasing rate is fast at high propane concentrations because the deposition reaction rate is proportional to the concentration of propane. For the same reason, the time changes of porosities in Fig. 4 decrease rapidly at high concentrations of propane. Furthermore, porosities at z=0 in Fig. 4(a) decrease more rapidly than those at z=0.5 L in Fig. 4(b).

The slope of the curve, i.e., deposition rate, at 30% in Fig. 4(a) increases a little with time. This is due to the increase of the lateral surface area of fibers. Usually, the rate of deposition is proportional to surface area and porosity. So the deposition rate decreases with time because of the decrease of the porosity among fibers and increases with time because of the increase of the lateral surface area of fibers. So the phenomenon that the slope of the curve increase with time at 30% propane means that the increasing deposition rate due to the increasing surface area becomes a little big compared with the decreasing rate due to the decreasing porosity.

Porosity distributions in the preform at different inlet concentrations of propane at 20 hr are in Fig. 5. The porosities at low concentrations of propane change very little compared with those at high concentrations. This means that a uniform deposition is obtained at a low concentration, i.e., a slow reaction rate.

Likewise, the amounts of deposition per unit mass of the preform in Fig. 6 change considerably with the inlet concentration of propane. It seems that the deposition amount increases in proportional to the increase of the inlet concentration. This is because the rate of deposition is a first order on the concentration of propane. Curves of the amount of deposition increase almost linearly with time. This means that the effect of the increase of the lateral surface area of fibers is negligible or offset by the effect of decrease of porosity, because, as mentioned before, the rate of deposition is proportional to surface area and porosity.

3. Effects of the Reaction Temperature

Distributions of porosity at 10 hr at different temperatures are in Fig. 7. The fraction of propane decreases rapidly at high reaction temperatures and near the pore entrances, since the consumption rate of propane is high at high temperatures. The graph shows that propane depletes almost completely and leaves nothing near pore exits at high temperatures, such as 930 and 950 °C.

It can be concluded with this graph that changes of porosity in

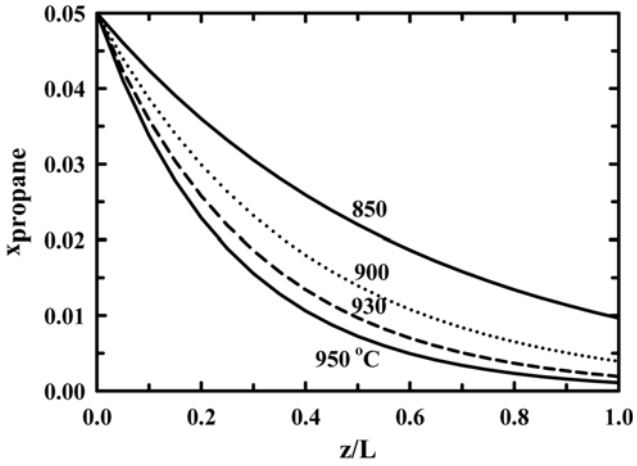

Fig. 7. Distributions of propane at 10 hr for the different reaction temperatures.

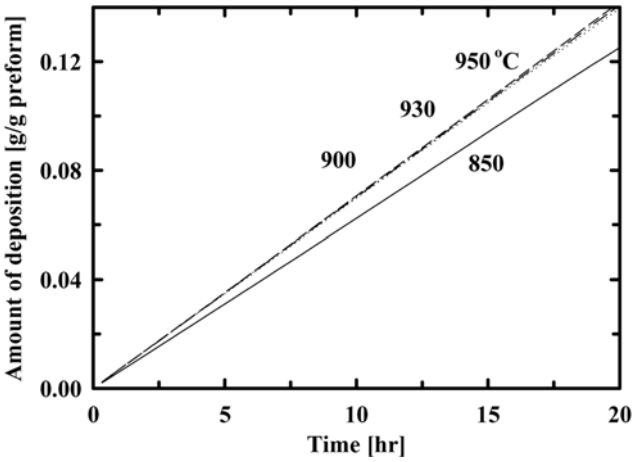

Fig. 9. Time changes of the amount of deposition at different reaction temperatures.

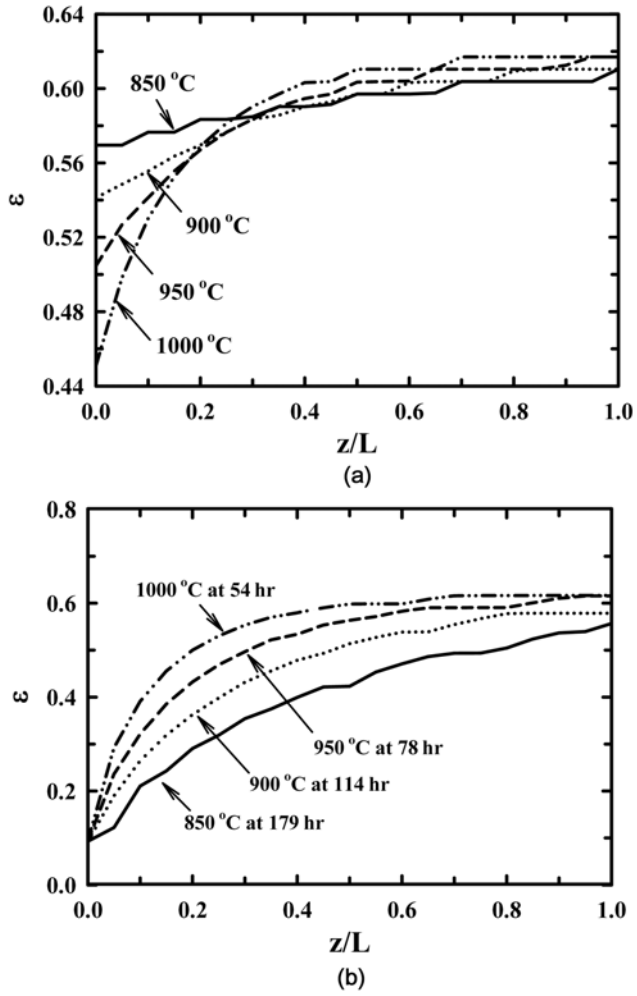

Fig. 8. Distributions of porosity for the different reaction temperatures (a) at 20 hr and (b) at the time of plugging pore entrances.

the preform with time at a low temperature would be smaller than those at a high temperature. Additionally, it can be said that a uniform deposition in the preform would be obtained at a low deposition temperature.

Distributions of porosity at 20 hr for the different reaction temperatures are in Fig. 8(a). The porosities near pore entrances at high temperatures are smaller than those at low temperatures, because the deposition rate is fast at high temperatures. However, the porosities near pore exits at high temperatures are greater than those at low temperatures, because propane is almost depleted near pore exits at high temperatures as shown in Fig. 7.

Distributions of porosity at the time of plugging pore entrances for the different reaction temperatures are in Fig. 8(b). Reversions of curves in Fig. 8(a) disappear in Fig. 8(b). At high temperatures, propane is almost depleted near pore exits and the reaction time is short because of the early plugging pore entrances. The times of plugging pore entrances at 850, 900, 950, and 1,000 °C are 179, 114, 78, and 54 hr, respectively. Fig. 8(a) and (b) are other exhibitions that a uniform deposition is obtained at a low temperature.

Time changes of the amount of deposition in the preform at different temperatures are in Fig. 9. Actually, the usual deposition curves increase rapidly at first and slowly later because of the diffusion limit due to the decrease of porosity. However, the amounts of deposition in Fig. 9 increase almost linearly and do not decrease with time. This can be explained as follows. Effects of the increase of the diffusion limit could be compensated with those of the increase of the surface area.

Additionally, curves at 900, 930, and 950 °C in Fig. 9 overlap in one curve, because of the depletion of propane near pore exits. At low temperatures, the deposition rate is slow. However, concentrations of propane near pore exits are great at low temperatures. So the low deposition rate at a low temperature is covered with a high propane concentration near exits. Thus the curves at 900, 930, and 950 °C in Fig. 9 could overlap in one curve.

4. Effects of the Reaction Rate Constant

How the distributions of propane in the preform depend on the size of the reaction rate constant (k_s) is shown in Fig. 10. As expected, when k_s is large, the consumption rate of propane is high and the slope of the distribution curve appears large. Propane depletes almost completely at 0.6 L with $30k_s$.

Distributions of porosity at 20 hr for the different reaction rate constants are in Fig. 11. Porosity dependences on the size of k_s in

this figure show a similar behavior as those on the temperature in Fig. 8(a). When k_s is large, porosities near pore entrances are small and those near pore exits are large, because propane is almost depleted near pore exits when k_s is large as shown in Fig. 10. This is another evidence that a uniform deposition can be obtained when the reaction is slow.

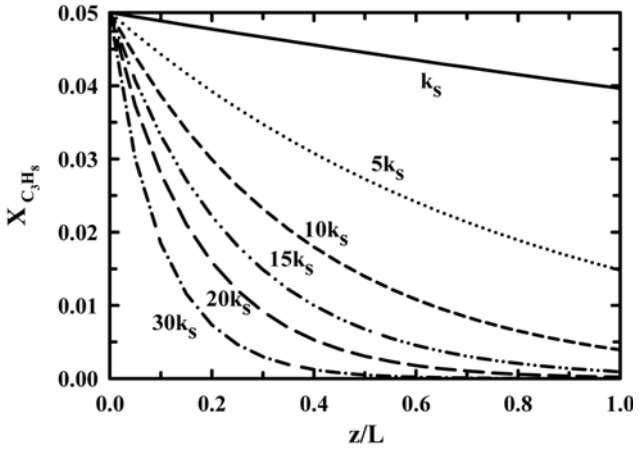

Fig. 10. Distributions of propane in the preform for the different reaction rate constants at 5% propane and 900 °C.

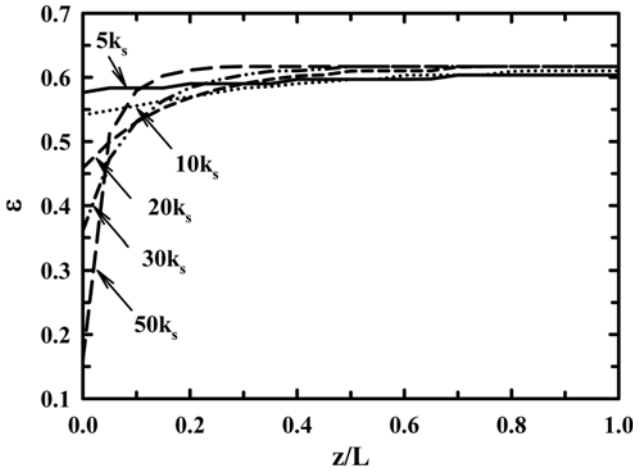

Fig. 11. Distributions of porosity at 20 hr for the different deposition rate constants at 900 °C and with 5% propane.

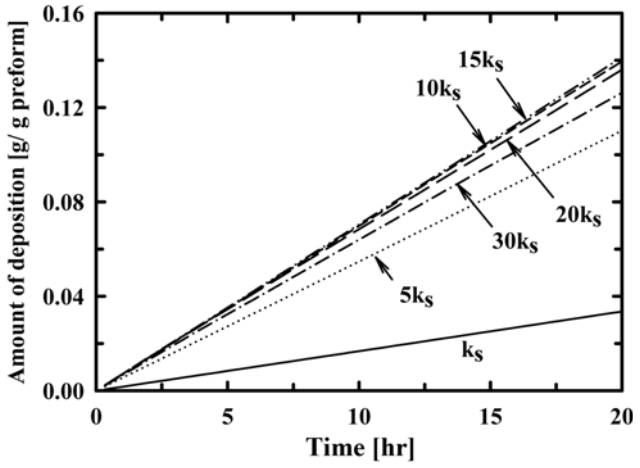

Fig. 12. Time changes of the amount of deposition for the different deposition rate constants at 900 °C and 5% propane.

Time changes of the amount of deposition at different reaction rate constants are in Fig. 12. Time changes of the amount of deposition dependence on k_s in this figure show a different behavior from the porosity distribution dependence on k_s in Fig. 11. Curves of the amount of deposition usually increase rapidly at first and slowly later because of the diffusion limit due to the decrease of the porosity. However, the slopes of curves in Fig. 12 seem almost constant; they increase almost linearly. This will be explained in the same way as done for the effect of reaction temperature. Effects of the increase of the diffusion limit could be compensated with those of the increase of the surface area.

The amount of deposition increases as k_s becomes $15k_s$. However, it decreases as $15k_s$ becomes $20k_s$ and $30k_s$. This is due to the depletion of propane in the middle of the preform at large k_s's as shown in Fig. 10.

5. Effects of the Gas Flow Rate and the Initial Porosity of the Preform

Effects of the gas flow rate and the initial porosity are shown in

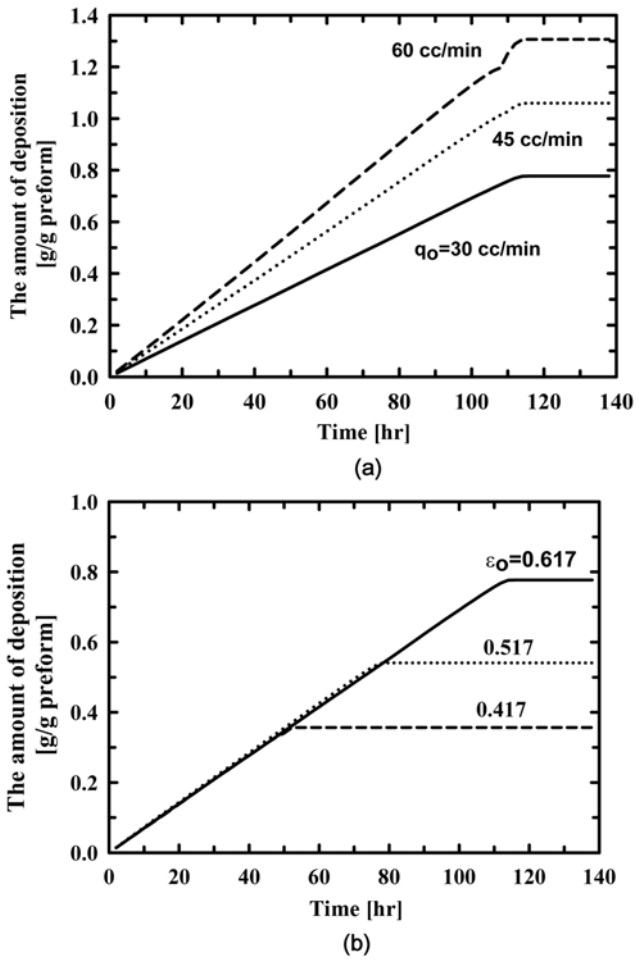

Fig. 13. Time changes of the amount of deposition (a) for the different gas flow rates and (b) for the different initial porosities of the preform. Other conditions: 900 °C and 5% propane.

Fig. 13. As the gas flow rate and the initial porosity increase, the amount of deposition increases. When the gas flow rate increases, the plugging times remain constant, because the deposition reaction rate is a function of the concentration and the concentration at pore entrances are constant. However, when the initial porosity of the preform increases, the time of plugging pore entrances extends as shown in Fig. 13(b), since the size of pore entrances becomes large as the porosity increases.

CONCLUSIONS

Modeling studies of the preparation of C/C composites by the pyrolysis of propane have been carried out. Experimental data were fitted with the modeling calculations using the reaction rate constant reported in the reference. An adjusted reaction rate constant was obtained. Effects of parameters of the deposition process were analyzed with this rate constant and the following conclusions were obtained.

The deposition rate decreases due to the decrease of porosity and the depletion of propane in the middle of the preform. However, this was compensated with the increase of the lateral surface area of fibers.

It was confirmed with the results of the numerical modeling that a low temperature, a low concentration, and a small reaction rate constant are necessary for a uniform infiltration.

As the gas flow rate and the initial porosity of the preform increase, the amount of deposition increases. Furthermore, if the initial porosity of the preform increases, the time of plugging pore entrances extends.

ACKNOWLEDGEMENT

This work was supported by the Korea Science and Engineering Foundation (KOSEF grant No. R01-2008-000-21103-0) funded by the Korean government. This work was also supported by the 2010 Hongik University research fund.

NOMENCLATURE

A : cross-sectional area of the perform [cm^2]
C : concentration of A, propane [mol/cm^3]
D : amount of deposition per unit cross-sectional area of the preform
k : first order (surface deposition) reaction rate constant [cm/s]
L : height of the preform
M : molecular weight
Q : volumetric flow rate [cm^3/s]
q : mole number of carbon deposited from 1 mole of propane
R : gas constant, 1.987 [cal/gmol K]
r : fiber radius [cm]
T : reaction temperature [K]
W : number of fibers in a unit cross-sectional area of the perform [$\#/cm^2$]
z : z-axis

Greek Letters

ε : porosity
υ : stoichiometric coefficient in Eq. (1)
ρ : density of deposited carbon [g/cm^3]

Subscripts

A : gaseous species that enter the reactor
f : fiber
m : deposited carbon
o : initial
s : surface
z : z-direction, gas flow direction

REFERENCES

1. P. Delhaes, *Carbon*, **40**, 641 (2002).
2. W. Zhang and K. J. Hüttinger, *Compos. Sci. Technol.*, **62**, 1947 (2002).
3. N. Birakayala and E. A. Evans, *Carbon*, **40**, 675 (2002).
4. K. Norinaga and O. Deutschmann, *Ind. Eng. Chem. Res.*, **46**, 3547 (2007).
5. C. A. Nannetti, B. Riccardi, A. Ortona, A. La Barbera, E. Scafea and G. Vekinis, *Nucl. Mater.*, **307**, 1196 (2002).
6. S. M. Gupte and J. A. Tsamopoulos, *J. Electrochem. Soc.*, **136**, 555 (1989).
7. G. Y. Chung, B. J. McCoy, J. M. Smith and D. E. Cagliostro, *AIChE J.*, **39**, 1834 (1993).
8. G. Y. Chung, B. J. McCoy, J. M. Smith and D. E. Cagliostro, *Chem. Eng. Sci.*, **47**, 311 (1992).
9. G. Y. Chung and B. J. McCoy, *J. Am. Ceram. Soc.*, **74**, 746 (1991).
10. C. W. Kim, M. S. Cho and G. Y. Chung, *Korean Chem. Eng. Res.*, **34**, 443 (1996).
11. H. J. Li, K. Y. Jiang and K. Z. Li, *Mater. Lett.*, **57**, 2366 (2003).
12. K. Jiang, H. Li and M. Wang, *Mater. Lett.*, **54**, 419 (2002).
13. R. Lacroix. R. Fournet, I. Ziegler and P. M. Marquaire, *Carbon*, **48**, 132 (2010).
14. H. Kim, G. Y. Chung, H. H. Koo and W. H. Baek. *Korean J. Chem. Eng.*, **21**, 929 (2004).
15. T. A. Langhoff and E. Schnack, *Chem. Eng. Sci.*, **63**, 3948 (2008).
16. J. Ibrahim and S. Paolucci, *Carbon*, **49**, 915 (2011).
17. I. Ziegler, R. Fournet and P. M. Marquaire, *J. Anal. Appl. Pyrol.*, **73**, 107 (2005).
18. S. Vaidyaraman, W. J. Lackey and P. K. Agrawal, *Carbon*, **34**, 609 (1996).
19. P. A. Tesner, *Chemistry and physics of carbon*, Edited by P. A. Thrower, **9**, 173 (1973).